

Highly Efficient Copper-Mediated Atom-Transfer Radical Addition (ATRA) in the Presence of Reducing Agent

William T. Eckenhoff,^[a] Sean T. Garrity,^[a] and Tomislav Pintauer*^[a]

Keywords: Catalysis / Copper / ATRA / Reducing agent

The synthesis, characterization and exceptional activity of $\text{Cu}^{\text{I}}(\text{TPMA})\text{Br}$ [TPMA = tris(2-pyridylmethyl)amine] and $[\text{Cu}^{\text{II}}(\text{TPMA})\text{Br}][\text{Br}]$ complexes in ATRA reactions of polybrominated compounds to alkenes in the presence of reducing agent (AIBN) was reported. $[\text{Cu}^{\text{II}}(\text{TPMA})\text{Br}][\text{Br}]$, in conjunction with AIBN, effectively catalyzed ATRA reactions of CBr_4 and CHBr_3 to alkenes with concentrations between 5 and 100 ppm, which is the lowest number achieved in copper-mediated ATRA. The molecular structure of $\text{Cu}^{\text{I}}(\text{TPMA})\text{Br}$ indicated that the complex was pseudo-pentacoordinate in the solid state due to the coordination of TPMA [$\text{Cu}^{\text{I}}\text{-N}$: 2.1024(15), 2.0753(15), 2.0709(15) and 2.4397(14) Å] and bromide anion to the copper(I) center [$\text{Cu}^{\text{I}}\text{-Br}$ 2.5088(3) Å]. Variable temperature ^1H NMR and cyclic voltammetry studies confirmed the equilibrium between $\text{Cu}^{\text{I}}(\text{TPMA})\text{Br}$ and $[\text{Cu}^{\text{I}}(\text{TPMA})(\text{CH}_3\text{CN})][\text{Br}]$, indicating some degree of halide anion dissociation in solution. The coordination of the bro-

midate anion to the $[\text{Cu}^{\text{I}}(\text{TPMA})]^+$ cation resulted in a formation of much more reducing $\text{Cu}^{\text{I}}(\text{TPMA})\text{Br}$ complex ($E_{1/2} = -720$ mV vs. Fc/Fc^+) than the corresponding ClO_4^- ($E_{1/2} = -422$ mV vs. Fc/Fc^+) and PF_6^- ($E_{1/2} = -421$ mV vs. Fc/Fc^+) analogues. In $[\text{Cu}^{\text{II}}(\text{TPMA})\text{Br}][\text{Br}]$, the Cu^{II} atom was coordinated by four nitrogen atoms [$\text{Cu}^{\text{II}}\text{-N}_{\text{eq}}$ 2.073(2) Å and $\text{Cu}^{\text{II}}\text{-N}_{\text{ax}}$ 2.040(3) Å] from TPMA ligand and a bromine atom [$\text{Cu}^{\text{II}}\text{-Br}$ 2.3836(6) Å]. The overall geometry of the complex was distorted trigonal bipyramidal. $\text{Cu}^{\text{I}}(\text{TPMA})\text{Br}$ and $[\text{Cu}^{\text{II}}(\text{TPMA})\text{Br}][\text{Br}]$ complexes showed similar structural features from the point of view of TPMA coordination. The only more pronounced difference in the TPMA coordination to the copper center was observed in the shortening of $\text{Cu}\text{-N}_{\text{ax}}$ bond length by approximately 0.400 Å on going from $\text{Cu}^{\text{I}}(\text{TPMA})\text{Br}$ to $[\text{Cu}^{\text{II}}(\text{TPMA})\text{Br}][\text{Br}]$.

(© Wiley-VCH Verlag GmbH & Co. KGaA, 69451 Weinheim, Germany, 2008)

Introduction

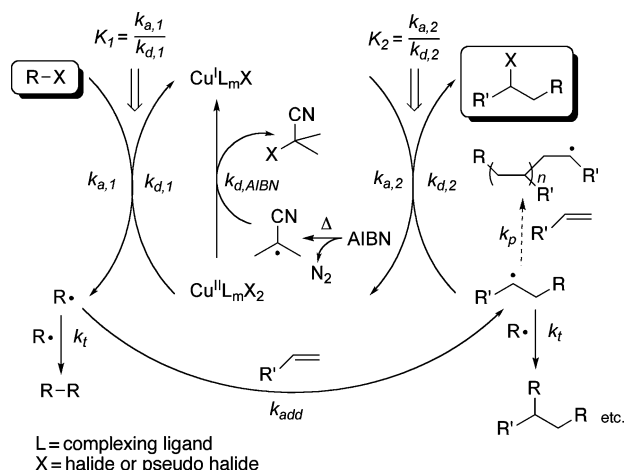
The addition of halogenated compounds to carbon-carbon double (or triple) bonds through a radical process is one of the fundamental reactions in organic chemistry.^[1,2] It was first reported in the early 1940s in which halogenated methanes were directly added to olefinic bonds in the presence of radical initiators or light.^[3,4] Today, this reaction is known as the Kharasch addition or atom-transfer radical addition (ATRA),^[5] and it is typically catalyzed by transition metal complexes of Ru, Fe, Ni and Cu.^[6-9] Although transition metal catalyzed ATRA can be applied to a variety of halogenated substrates and alkenes, the principal drawback of this useful synthetic tool until recently remained the large amount of catalyst required to achieve the high selectivity towards monoadduct. The solution to this problem has been found for atom transfer radical polymerization (ATRP),^[10-21] which originated from ATRA. These new processes termed initiators for continuous activator regeneration (ICAR)^[22] and activators regenerated by electron transfer (ARGET)^[23,24] utilize copper(II) complexes

which are continuously reduced to copper(I) complexes in the presence of phenols, glucose, ascorbic acid, hydrazine, tin(II) 2-ethylhexanoate and radical initiators. With ICAR ATRP, controlled synthesis of poly(styrene) and poly(methyl methacrylate) can be implemented with catalyst concentrations between 10 and 50 ppm.^[22] This technique for catalyst regeneration has recently been utilized with great success in ATRA reactions catalyzed by $[\text{Cp}^*\text{Ru}^{\text{III}}\text{Cl}_2(\text{PPh}_3)]$ complex.^[25,26] In the case of ATRA of CCl_4 to olefins in the presence of AIBN, TONs as high as 44500 were obtained.^[25] We have also applied this technique in copper mediated ATRA utilizing $\text{Cu}^{\text{I}}(\text{TPMA})\text{Cl}$ and $[\text{Cu}^{\text{II}}(\text{TPMA})\text{Cl}][\text{Cl}]$ complexes [TPMA = tris(2-pyridylmethyl)amine].^[27] TPMA ligand was chosen for the study because its complexation to $\text{Cu}^{\text{I}}\text{X}$ (X = Cl or Br) results in a formation of one of the most active catalysts in copper mediated ATRP.^[28-30] The maximum activity in the addition of CCl_4 to alkenes was achieved with the catalyst to olefin ratio of 1:10,000, resulting in TONs of 7,200 for 1-hexene and 6,700 for 1-octene.

The underlying principle of catalyst regeneration in the presence of reducing agent in ATRA is shown in Scheme 1. The mechanism is modified from the well established free radical mechanism operating in metal-catalyzed ATRA reactions.^[7,31-34] In order to increase the chemoselectivity towards the monoadduct, the following general guidelines

[a] Department of Chemistry and Biochemistry, Duquesne University, 600 Forbes Avenue, 308 Mellon Hall, Pittsburgh, PA 15282, USA
Fax: +1-412-396-5683
E-mail: pintauert@duq.edu

need to be met: (a) radical concentration must be low in order to suppress radical termination reactions [activation rate constant ($k_{a,1}$ and $k_{a,2}$) \ll deactivation rate constant ($k_{d,1}$ and $k_{d,2}$)], (b) further activation of the monoadduct should be avoided ($k_{a,1} \gg k_{a,2}$) and (c) the formation of oligomers/polymers should be suppressed {rate of transfer [$k_{d,2}(\text{Cu}^{\text{II}}\text{L}_m\text{X})$] \gg rate of propagation [$k_p(\text{alkene})$]}. If a large excess of alkyl halide is used relative to copper(I) complex, the equilibrium $K_1 = k_{a,1}/k_{d,1}$ will be shifted towards the right hand side and, as a result of irreversible radical coupling reactions, all of the copper(I) complex will be converted into the corresponding copper(II) complex. To compensate for this unavoidable side reaction in ATRA, a reducing agent such as the radical initiator 2,2'-azobis(2-methylpropionitrile) (AIBN) is added to the reaction mixture. The slow decomposition of AIBN provides a constant source of radicals, which continuously reduce copper(II) to copper(I) complex. Copper(I) complex is needed for the activation of alkyl halide (R-X). Furthermore, the efficient regeneration of the copper(I) complex by reducing agent enables ATRA reactions to be conducted starting with the air-stable copper(II) complex.^[27] Similar observations were also made in the case of [Cp* $\text{Ru}^{\text{II}}\text{Cl}_2(\text{PPh}_3)$] complex.^[25,26] The outlined methodology to decrease the amount of metal catalyst in ATRA reactions could have a significant impact in radical syntheses of natural products, pharmaceutical drugs and other complex molecules, which are currently predominantly conducted utilizing stoichiometric amounts of organotin and organosilane reagents.^[35-37] In conjunction with the reduced amount of metal catalyst, the other potential advantage of transition-metal-catalyzed ATRA is that the resulting product contains a halide group, which can be easily reduced, eliminated, displaced or converted to a Grignard reagent.



Scheme 1. Proposed mechanism for copper(I) regeneration in the presence of reducing agent (AIBN) during ATRA process.

In this article, we report on the synthesis, characterization and exceptional activity of $\text{Cu}^{\text{I}}(\text{TPMA})\text{Br}$ and $[\text{Cu}^{\text{II}}(\text{TPMA})\text{Br}][\text{Br}]$ complexes in ATRA reactions of polybrominated compounds to alkenes in the presence of a reducing agent (AIBN).

Results and Discussion

ATRA of CHBr_3 and CBr_4 to Alkenes

The addition of CBr_4 to simple olefins (1-hexene, 1-octene and 1-decene) in the presence of the reducing agent AIBN, but without the $\text{Cu}^{\text{I}}(\text{TPMA})\text{Br}$ complex, proceeded very efficiently at 60 °C and the desired monoadduct was formed in quantitative yields (Table 1). These results are not surprising because of the known ability of CBr_4 to function as a very efficient chain-transfer agent.^[38,39] In the case of methyl acrylate (Entry 4) and styrene (Entry 5), quantitative conversions were also observed, however, the decreased yield of the monoadduct was mostly due to the formation of oligomers/polymers as a result of the presence of free radical initiator. Similar reactions in the presence of CHBr_3 yielded very low amounts of the monoadduct in the case of 1-hexene (8%, Entry 6), 1-octene (9%, Entry 7) and 1-decene (8%, Entry 8) or none in the case of methyl acrylate (Entry 9) and styrene (Entry 10). For the latter two alkenes, the major products were oligomers/polymers. In the absence of AIBN, ATRA of CBr_4 and CHBr_3 with the $\text{Cu}^{\text{I}}(\text{TPMA})\text{Br}$ to alkene ratios between 1:500 and 1:10000 did not yield the desired monoadduct, despite the high activity of the complex in ATRP.^[28-30] The principle reason was the complete deactivation of the copper(I) complex to the corresponding copper(II) complex, consistent with the proposed mechanism shown in Scheme 1.

Table 1. Addition of polybrominated compounds to alkenes in the presence of AIBN.

Entry ^[a]	Alkene	RBr	% Conversion	% Yield
1	1-hexene	CBr_4	≈100	≈100
2	1-octene	CBr_4	≈100	≈100
3	1-decene	CBr_4	≈100	≈100
4	methyl acrylate	CBr_4	≈100	32
5	styrene	CBr_4	99	72
6	1-hexene	CHBr_3	10	8
7	1-octene	CHBr_3	9.5	9
8	1-decene	CHBr_3	11	8
9	methyl acrylate	CHBr_3	99	0
10	styrene	CHBr_3	41	0

[a] All reactions were performed in CH_3CN at 60 °C for 24 h with $[\text{R}-\text{Br}]_0:[\text{alkene}]_0:[\text{AIBN}]_0 = 4:1:0.05$. The yield is based on the formation of monoadduct and was determined by ^1H NMR using anisole or toluene as internal standard.

ATRA of CHBr_3 and CBr_4 to Alkenes Catalyzed by $[\text{Cu}^{\text{II}}(\text{TPMA})\text{Br}][\text{Br}]$ in the Presence of AIBN

Table 2 shows the results for the ATRA of polybrominated compounds to alkenes catalyzed by $[\text{Cu}^{\text{II}}(\text{TPMA})\text{Br}][\text{Br}]$ complex in the presence of a reducing agent AIBN. The reaction conditions were optimized in such a way as to achieve maximum conversion of the alkene and high yield of the monoadduct. For methyl acrylate, a significant improvement in the yield of the monoadduct was achieved using $[\text{Cu}^{\text{II}}(\text{TPMA})\text{Br}][\text{Br}]$ to methyl acrylate ratios of 1:200000 (81%, Entry 1) and 1:100000 (94%, Entry 2).

Furthermore, using identical reaction conditions, the complete conversion of styrene was also achieved with the main product being the desired monoadduct (95% Entry 3 and 99% Entry 4). These results clearly indicate that the slow decomposition of AIBN provides a constant source of radicals, which continuously reduce $[\text{Cu}^{\text{II}}(\text{TPMA})\text{Br}][\text{Br}]$ complex to $\text{Cu}^{\text{I}}(\text{TPMA})\text{Br}$, which is needed to homolytically cleave the R–Br bond.

Table 2. ATRA of polybrominated compounds to alkenes catalyzed by $[\text{Cu}^{\text{II}}(\text{TPMA})\text{Br}][\text{Br}]$ in the presence of AIBN.

Entry ^[a]	Alkene	RBr	[Alk.] ₀ /[Cu ^{II}] ₀	% Conv.	% Yield ^[b]
1	methyl acrylate	CBr ₄	200000:1	≈100	81 (76) ^[c]
2			100000:1	≈100	94
3	styrene	CBr ₄	200000:1	≈100	95 (86) ^[c]
4			100000:1	99	99
5	methyl acrylate	CHBr ₃	10000:1	≈100	11 (11) ^[c]
6			5000:1	≈100	23
7			1000:1	≈100	57
8			500:1	≈100	66
9	styrene	CHBr ₃	10000:1	≈100	70
10			5000:1	≈100	77
11			1000:1	≈100	92
12	1-hexene	CHBr ₃	10000:1	67	61 (59) ^[c]
13	1-octene	CHBr ₃	10000:1	75	69 (54) ^[c]
14	1-decene	CHBr ₃	10000:1	74	63 (64) ^[c]

[a] All reactions were performed in bulk at 60 °C for 24 h with $[\text{R}-\text{Br}]_0/[\text{alkene}]_0/[\text{AIBN}]_0 = 4:1:0.05$, except reactions for Entries 1–4 which were performed in CH_3CN . [b] The yield is based on the formation of monoadduct and was determined by ¹H NMR using anisole or toluene as internal standard. [c] Isolated yield after column chromatography.

As indicated in Table 2, the methodology for the copper(I) regeneration in ATRA in the presence of the reducing agent AIBN worked very well for the less active bromoform. Relatively high yields of the monoadduct were obtained in ATRA of CHBr_3 to methyl acrylate (Entry 7 and 8) and styrene (Entry 10 and 11), but with much higher catalyst loadings. Further decrease in the amount of catalyst for both monomers resulted in a decrease in the yield of the monoadduct. The decrease in the yield of monoadduct was mostly due to the formation of oligomers/polymers, which can be attributed to (a) insufficient trapping of radicals generated from AIBN by the copper(II) complex and (b) further activation of the monoadduct by the copper(I) complex (more pronounced in the case of methyl acrylate). In the ATRA of CHBr_3 to 1-hexene (Entry 12), 1-octene (Entry 13) and 1-decene (Entry 14), moderate yields of the monoadduct can be attributed to incomplete alkene conversions. Furthermore, the conversions of the alkene for Entries 12–14 were relatively independent on the copper(II):alkene ratios between 1:500 and 1:10000, indicating that the rate of addition of CHBr_2 radicals to alkenes is slow. ATRA of CHBr_3 to alkenes (Entries 5–14, Table 2) yielded similar results in acetonitrile, indicating that an increase in solvent polarity did not significantly alter the catalytic performance of $[\text{Cu}^{\text{II}}(\text{TPMA})\text{Br}][\text{Br}]$.

The activity of $[\text{Cu}^{\text{II}}(\text{TPMA})\text{Br}][\text{Br}]$ complex in ATRA of polybrominated compounds to alkenes in the presence of AIBN, based on catalyst loading, conversion of alkene

and the yield of the monoadduct, is approximately 10 times higher than the activity of previously reported $[\text{Cu}^{\text{II}}(\text{TPMA})\text{Cl}][\text{Cl}]$ in the ATRA of polychlorinated compounds to alkenes. Also, for comparable monomers and alkyl halides, its activity is very close to the activity of $[\text{Cp}^*\text{Ru}^{\text{III}}\text{Cl}_2(\text{PPh}_3)]$ complex.^[25] $[\text{Cu}^{\text{II}}(\text{TPMA})\text{Br}][\text{Br}]$, in conjunction with AIBN, effectively catalyzes ATRA reactions of polybrominated compounds to alkenes with concentrations between 5 and 100 ppm, which is by far the lowest number achieved in copper mediated ATRA.^[9,27,40,41]

Synthesis and Characterization of $\text{Cu}^{\text{I}}(\text{TPMA})\text{Br}$

The high activity of $[\text{Cu}^{\text{I}}(\text{TPMA})\text{Br}]$ and $[\text{Cu}^{\text{II}}(\text{TPMA})\text{Br}][\text{Br}]$ complexes in ATRA can be explained in terms of increased values of the activation rate constant ($k_{a,1}$, Scheme 1) and the equilibrium constant for atom transfer ($K_1 = k_{a,1}/k_{d,1}$, Scheme 1), when compared to other copper(I) complexes with bidentate and tridentate nitrogen-based ligands and different counterions.^[42–45] The structural features of highly ATRP and now ATRA active $\text{Cu}^{\text{I}}\text{X}/\text{TPMA}$ (X = Cl and Br) complexes are still not fully understood.^[46] TPMA typically coordinates to the copper(I) complex in a tetradentate fashion, similarly to structurally related tris[2-(*N,N*-dimethylamino)ethyl]amine (Me_6TREN).^[47,48] However, the role of the counterion in these complexes is also very unclear. For example, in the crystal structure of $[\text{Cu}^{\text{I}}(\text{Me}_6\text{TREN})][\text{ClO}_4]$,^[48] the copper(I) atom was found to be distorted trigonal bipyramidal and it was coordinated by 4 nitrogen atoms from the Me_6TREN ligand [$\text{Cu}^{\text{I}}-\text{N}_{\text{eq}}$ 2.122(7) Å and $\text{Cu}^{\text{I}}-\text{N}_{\text{ax}}$ 2.200(14) Å] and an oxygen atom from the ClO_4^- anion [$\text{Cu}^{\text{I}}-\text{O}$ 3.53(1) Å]. In the case of $\text{Cu}^{\text{I}}\text{Br}/\text{Me}_6\text{TREN}$ complex, EXAFS studies have indicated several possible structures in solution which included $[\text{Cu}^{\text{I}}(\text{Me}_6\text{TREN})][\text{Br}]$, $[\text{Cu}^{\text{I}}(\text{Me}_6\text{TREN})][\text{Cu}^{\text{I}}\text{Br}_2]$ and $[\text{Cu}^{\text{I}}(\text{Me}_6\text{TREN}')\text{Br}]$ ($\text{Me}_6\text{TREN}'$ denotes a tricoordinate Me_6TREN).^[46,49–51] These structures were based on the validated assumption that the maximum coordination number of copper(I) should not exceed four.^[52] Recently, we have isolated a neutral $\text{Cu}^{\text{I}}(\text{TPMA})\text{Cl}$ complex, which was surprisingly pseudo-pentacoordinate.^[27] The copper(I) ion was coordinated by four nitrogen atoms with bond lengths of 2.0704(11), 2.0833(11) and 2.0888(11) Å for the equatorial Cu–N and 2.4366(11) Å for the axial Cu–N bonds and a chlorine atom with a bond length of 2.3976(4) Å.

The molecular structure of the $\text{Cu}^{\text{I}}(\text{TPMA})\text{Br}$ complex (Figure 1) was obtained by slow crystallization of $\text{Cu}^{\text{I}}\text{Br}/\text{TPMA}$ from THF/EtOH at –35 °C. The copper(I) center is also pseudo-pentacoordinate and the geometry of the complex is distorted trigonal bipyramidal. The copper(I) atom is coordinated by four nitrogen atoms with bond lengths of 2.1014(15), 2.0753(15), and 2.0709(15) Å for the equatorial Cu–N and 2.4397(14) Å for the axial Cu–N bonds and a Cu–Br bond length of 2.5088(3) Å. Furthermore, the copper(I) atom lies 0.538(6) Å below the least-squares plane

derived from N2, N3 and N4, towards the bromide ion. The molecule possesses near (noncrystallographic) three-fold symmetry with respect to the Cu–Br1 or Cu–N1 vector.

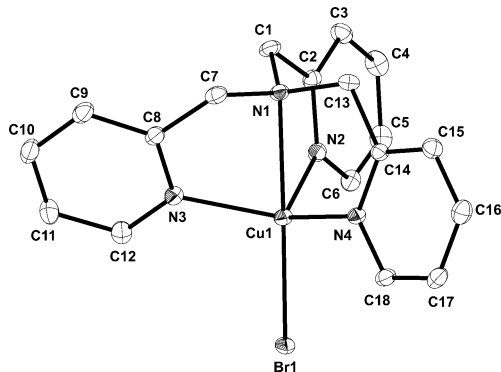


Figure 1. Molecular structure of $\text{Cu}^{\text{I}}(\text{TPMA})\text{Br}$, shown with 30% thermal probability ellipsoids. H atoms have been omitted for clarity. Selected distances [Å] and angles [°]: Cu1–N1 2.4397(14), Cu1–N2 2.1024(15), Cu1–N3 2.0753(15), Cu1–N4 2.0709(15), Cu1–Br1 2.5088(3), N4–Cu1–N3 120.51(6), N4–Cu1–N2 112.40(6), N3–Cu1–N2 107.61(6), N4–Cu1–N1 75.37(5), N3–Cu1–N1 74.86(5), N2–Cu1–N1 74.80(5), N1–Cu1–Br1 179.14(3).

The proton resonances in the ^1H NMR spectrum of the $\text{Cu}^{\text{I}}(\text{TPMA})\text{Br}$ complex in $(\text{CD}_3)_2\text{CO}$ at room temperature (Figure 2) are very broad, indicating a fluxional system. However, on cooling to 220 K, the resonances due to the coordinated TPMA ligand become very well resolved. Only one set of resonances for the protons in the TPMA ligands were observed which is consistent with near threefold symmetry observed in the solid-state structure of $\text{Cu}^{\text{I}}(\text{TPMA})\text{Br}$ complex. Because TPMA coordinates to the copper(I) center through four nitrogen atoms, hydrogen atoms that are close to the coordinated nitrogen atoms should be significantly deshielded relative to the free ligand. This was indeed observed. The chemical shift of the hydrogen atom next to the nitrogen atom in the pyridine ring (H^1 , Figure 2) at 220 K moves approximately 0.60 ppm downfield relative to free TPMA. Such downfield shift in proton resonances between 0.50 and 0.70 ppm is typically observed in copper(I) complexes with nitrogen-based ligands.^[53–56] Similarly, the downfield shift of the methylene protons in TPMA (H^5 , Figure 2) by 0.10 ppm also indicates coordination. Much smaller downfield shift for methylene protons (H^5) when compared to H^1 in coordinated TPMA is also consistent with the solid-state structure of the $\text{Cu}^{\text{I}}(\text{TPMA})\text{Br}$ complex. In $\text{Cu}^{\text{I}}(\text{TPMA})\text{Br}$, the distance between the central nitrogen atom and the copper(I) center is on average 0.360 Å longer than the distance between the copper(I) center and the nitrogen atom from the pyridine ring. Consequently, the deshielding effect for the methylene protons (H^5) should be less than for the pyridine proton (H^1), which was observed. The resonances for H^2 and H^3 protons in $\text{Cu}^{\text{I}}(\text{TPMA})\text{Br}$ are only slightly shielded upon coordination ($\Delta\delta = 0.12$ and 0.05 ppm, respectively). Furthermore, the resonance for the H^4 proton moves approximately 0.32 ppm upfield upon TPMA coordination to the copper(I) center.

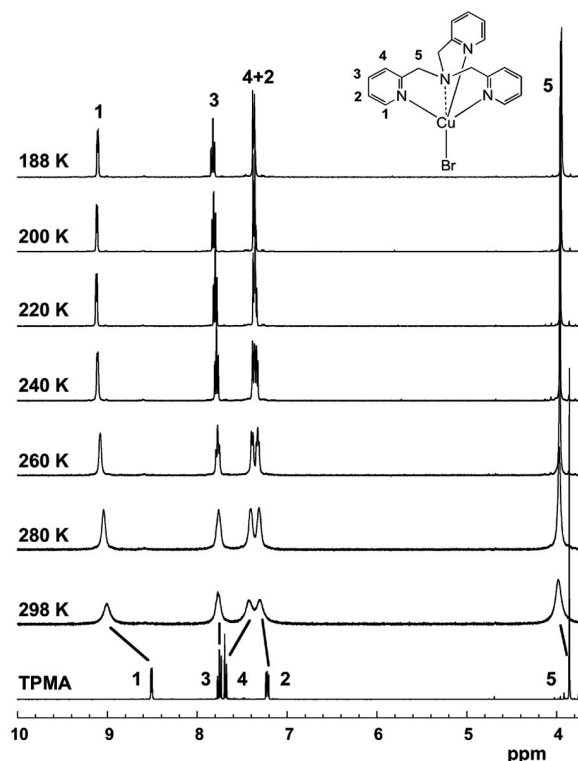
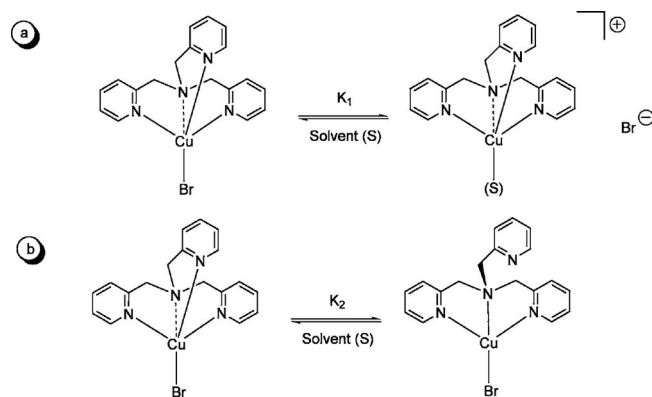


Figure 2. Variable-temperature ^1H NMR spectra [400 MHz, $(\text{CD}_3)_2\text{CO}$] of the $\text{Cu}^{\text{I}}(\text{TPMA})\text{Br}$ complex.

The broadened resonances in the solution ^1H NMR spectra of $\text{Cu}^{\text{I}}(\text{TPMA})\text{Br}$ (260–298 K) in $(\text{CD}_3)_2\text{CO}$ could be induced by the occurrence of the fluxional processes such as the ligand dissociation, which are well known in copper(I) complexes with nitrogen-containing ligands.^[57–59] In the case of the tetradentate TPMA ligand, the dissociation and association of the pyridine nitrogen atoms has been proposed in the previous studies, as well as the possibility for the formation of dimers in which each copper(I) ion is ligated with two pyridine nitrogen atoms and one tertiary amine nitrogen atom of a single TPMA and one pyridine nitrogen atom of the second adjacent TPMA ligand.^[60,61] The ^1H NMR spectra of $\text{Cu}^{\text{I}}(\text{TPMA})\text{Br}$ in Figure 2 are not consistent with the dimer formation because such coordination environment would result in two chemically inequivalent methylene groups. Furthermore, the association/dissociation of the pyridine atoms in TPMA ligand (Scheme 2) appears to be the minor dynamic process because significant deshielding effects would have been observed in the variable temperature ^1H NMR studies. For example, the chemical shift of the hydrogen atom next to the nitrogen atom in the pyridine ring of the TPMA ligand (H^1 , Figure 2) becomes deshielded by approximately 0.10 ppm in the temperature range 298–188 K. In order to test the possibility for Br^- dissociation from the $\text{Cu}^{\text{I}}(\text{TPMA})\text{Br}$ complex, NMR experiments were performed in the presence of externally added source of Br^- anions, such as tetrabutylammonium bromide (TBABr). In the presence of 1.0 equiv. of TBABr, the room temperature ^1H NMR

spectrum of $\text{Cu}^{\text{I}}(\text{TPMA})\text{Br}$ appeared sharper and resembled the spectrum of $\text{Cu}^{\text{I}}(\text{TPMA})\text{Br}$ at 260 K in the absence of TBABr. This indicates that the broadening in the ^1H NMR spectra of $\text{Cu}^{\text{I}}(\text{TPMA})\text{Br}$ (260–298 K) is induced by the dissociation of the Br^- anions to generate $[\text{Cu}^{\text{I}}(\text{TPMA})]^+[\text{Br}]^-$. Furthermore, variable temperature experiments performed in CD_3CN (230–298 K) also indicated halide anion dissociation. Additionally, in the case of $\text{Cu}^{\text{I}}(\text{TPMA})\text{Br}$ complex in CD_3CN (99% D), we were able to observe the proton resonance for the coordinated CD_3CN , which progressively shifted from 2.13 ppm (298 K) to 2.35 ppm (230 K). At 230 K, only four resonances for the coordinated TPMA ligand were observed, indicating the formation of $[\text{Cu}^{\text{I}}(\text{TPMA})(\text{CH}_3\text{CN})][\text{Br}]$ complex in solution (Scheme 2). Copper(I) complexes with the TPMA ligand and its derivatives containing acetonitrile as the fifth ligand have been previously observed and structurally characterized.^[60] Quantifying the temperature and solvent dependence on the equilibrium constant for the bromide anion dissociation from $\text{Cu}^{\text{I}}(\text{TPMA})\text{Br}$ complex is the subject to future investigation in our laboratories. The study could provide much needed information in an ongoing debate on the nature of the atom transfer radical addition and polymerization from the point of view of concerted inner-sphere electron transfer process (ISET) or a two step process with an outer-sphere electron transfer (OSET).^[11,62,63]



Scheme 2. Proposed equilibria for $\text{Cu}^{\text{I}}(\text{TPMA})\text{Br}$ involving (a) halide anion and (b) pyridine nitrogen association/dissociation.

In order to further examine the coordination of the bromide anion to the $\text{Cu}^{\text{I}}(\text{TPMA})\text{Br}$ complex, cyclic voltammetry experiments were performed. Cyclic voltammetry has been extensively used in probing the catalytic activity of copper(I) complexes in ATRP/ATRA because the redox potential can be correlated with the equilibrium constant for atom transfer (K_{ATRA} or K_{ATRP} , Scheme 1).^[44,46,50,64] Figure 3 shows cyclic voltammograms of $[\text{Cu}^{\text{I}}(\text{TPMA})][\text{A}]$ ($\text{A} = \text{ClO}_4^-$, PF_6^- and Br^-) complexes in the presence of different supporting electrolytes in CH_3CN at room temperature. The electrochemical data are given in Table 3. The copper(I) complexes display single quasireversible redox behavior with $i_{\text{pa}}/i_{\text{pc}}$ varying from 0.91 to 1.08.

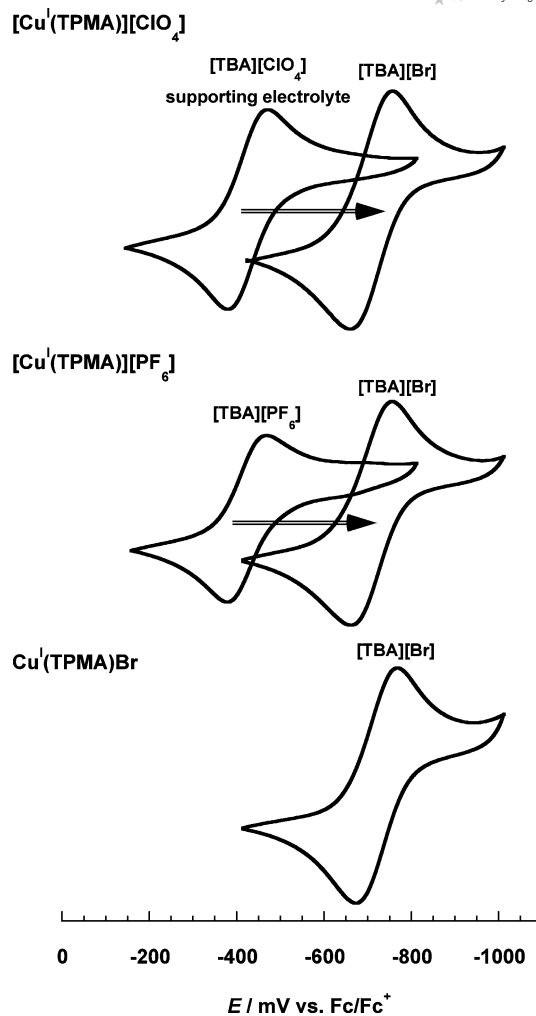


Figure 3. Cyclic voltammograms of $[\text{Cu}^{\text{I}}(\text{TPMA})][\text{A}]$ ($\text{A} = \text{ClO}_4^-$, PF_6^- and Br^-) in the presence of different supporting electrolytes in CH_3CN at room temperature. Spectra are presented with respect to Fc/Fc^+ couple.

Table 3. Cyclic voltammetry data for copper(I) complexes in CH_3CN .

Complex ^[a]	Supp. Elect.	$E_{1/2}$ [mV]	ΔE_p [mV]	$i_{\text{pa}}/i_{\text{pc}}$
$[\text{Cu}^{\text{I}}(\text{TPMA})][\text{ClO}_4^-]$	TBAClO ₄	-422	94	0.95
	TBABr	-706	97	0.92
$[\text{Cu}^{\text{I}}(\text{TPMA})][\text{PF}_6^-]$	TBAPF ₆	-421	88	0.94
	TBABr	-711	88	0.91
$\text{Cu}^{\text{I}}(\text{TPMA})\text{Br}$	TBABr	-720	93	1.08

[a] Potentials are reported vs. Fc/Fc^+ and were measured under the same electrochemical cell conditions.

Peak separations were all less than 100 mV at a scan rate of 100 mV/s. The $\text{Cu}^{\text{II}}/\text{Cu}^{\text{I}}$ reduction potentials measured for the copper(I) complexes are reported relative to the ferrocene-ferrocenium couple which was used as an external reference. The redox potentials for $[\text{Cu}^{\text{I}}(\text{TPMA})][\text{ClO}_4^-]/\text{TBAClO}_4$ (supporting electrolyte) and $[\text{Cu}^{\text{I}}(\text{TPMA})][\text{PF}_6^-]/\text{TBAPF}_6$ were determined to be $E_{1/2} = -422$ mV ($\Delta E_p = 94$ mV) and $E_{1/2} = -421$ mV ($\Delta E_p = 88$ mV) in CH_3CN , respectively. Changing the supporting electrolyte to TBABr

resulted in the shifting of cyclic voltammograms for both complexes by approximately 300 mV [$E_{1/2} = -706$ mV ($\Delta E_p = 97$ mV) for ClO_4^- and $E_{1/2} = -711$ mV ($\Delta E_p = 88$ mV) for PF_6^- complex, respectively]. Furthermore, as indicated in Figure 3, both voltammograms were nearly identical to the cyclic voltammogram of $\text{Cu}^{\text{I}}(\text{TPMA})\text{Br}$ complex using TBABr as the supporting electrolyte [$E_{1/2} = -720$ mV ($\Delta E_p = 93$ mV)]. Therefore, for both complexes, it is apparent that the bromide anion has coordinated to the $[\text{Cu}^{\text{I}}(\text{TPMA})]^+$ cation forming the $\text{Cu}^{\text{I}}(\text{TPMA})\text{Br}$ complex, confirming the reverse of the equilibrium shown in Scheme 2. These results also indicate that the coordination of the bromide anion to the $[\text{Cu}^{\text{I}}(\text{TPMA})]^+$ cation results in a formation of much more reducing $\text{Cu}^{\text{I}}(\text{TPMA})\text{Br}$ complex, when compared to ClO_4^- and PF_6^- analogues. Because previous studies by Matyjaszewski et al.^[44,46,50,64] have indicated that the K_{ATRP} or K_{ATRA} equilibrium constants correlate linearly with the $E_{1/2}$ values of the copper complexes [provided that copper(II) complexes have similar “halidophilicities” (K_{HP}) or the equilibrium constants for the heterolytic dissociation of the halide anion], one can assume that the $\text{Cu}^{\text{I}}(\text{TPMA})\text{Br}$ complex should be a better catalyst for ATRA/ATRP, then $[\text{Cu}^{\text{I}}(\text{TPMA})][\text{ClO}_4^-]$ or $[\text{Cu}^{\text{I}}(\text{TPMA})][\text{PF}_6^-]$. However, in the ATRA of CHBr_3 and CBr_4 to alkenes catalyzed by $[\text{Cu}^{\text{I}}(\text{TPMA})][\text{A}]$ ($\text{A} = \text{ClO}_4^-, \text{PF}_6^-$ and Br^-) similar catalytic activities were obtained. Therefore, apart from the redox potentials, additional factors must also contribute towards the equilibrium constant for atom transfer.

Synthesis and Characterization of $[\text{Cu}^{\text{II}}(\text{TPMA})\text{Br}][\text{Br}]$

The corresponding deactivator, $[\text{Cu}^{\text{II}}(\text{TPMA})\text{Br}][\text{Br}]$ was synthesized by reacting $\text{Cu}^{\text{II}}\text{Br}_2$ with the stoichiometric amount of TPMA. The same complex can be alternatively prepared by reacting $\text{Cu}^{\text{I}}(\text{TPMA})\text{Br}$ with excess alkyl halide (CBr_4 or CHBr_3). Figure 4 shows the molecular structure of the $[\text{Cu}^{\text{II}}(\text{TPMA})\text{Br}][\text{Br}]$ complex. In $[\text{Cu}^{\text{II}}(\text{TPMA})\text{Br}][\text{Br}]$, the Cu^{II} atom is coordinated by four nitrogen atoms [$\text{Cu}^{\text{II}}\text{-N}_{\text{eq}} 2.073(2)$ Å and $\text{Cu}^{\text{II}}\text{-N}_{\text{ax}} 2.040(3)$ Å] from the TPMA ligand and a bromine atom [$\text{Cu}^{\text{II}}\text{-Br} 2.3836(6)$ Å]. The overall geometry of the complex is distorted trigonal bipyramidal and the copper(II) atom is positioned 0.329(3) Å below the least-squares plane derived from the equatorial nitrogen atoms in TPMA. The N1, Cu1 and Br1 atoms lie on the crystallographic threefold rotation axis.

From the point of view of TPMA coordination, the structures of $\text{Cu}^{\text{I}}(\text{TPMA})\text{Br}$ and $[\text{Cu}^{\text{II}}(\text{TPMA})\text{Br}][\text{Br}]$ are very similar. In $\text{Cu}^{\text{I}}(\text{TPMA})\text{Br}$ complex, the average $\text{Cu}^{\text{I}}\text{-N}_{\text{eq}}$ bond length is 0.0100 Å longer than in $[\text{Cu}^{\text{II}}(\text{TPMA})\text{Br}][\text{Br}]$. The $\text{N}_{\text{ax}}\text{-Cu}\text{-N}_{\text{eq}}$ angles are very similar in both complexes, while the average angle in the plane $\text{N}_{\text{ax}}\text{-Cu}\text{-N}_{\text{ax}}$ is slightly larger in $[\text{Cu}^{\text{II}}(\text{TPMA})\text{Br}][\text{Br}]$ [$117.53(3)^\circ$] than in $\text{Cu}^{\text{I}}(\text{TPMA})\text{Br}$ [$113.51(10)^\circ$]. The only more pronounced difference in the TPMA coordination to the copper center can be seen in the shortening of $\text{Cu}\text{-N}_{\text{ax}}$ bond length by approximately 0.400 Å on going from $\text{Cu}^{\text{I}}(\text{TPMA})\text{Br}$ to $[\text{Cu}^{\text{II}}(\text{TPMA})\text{Br}][\text{Br}]$. Similar observations

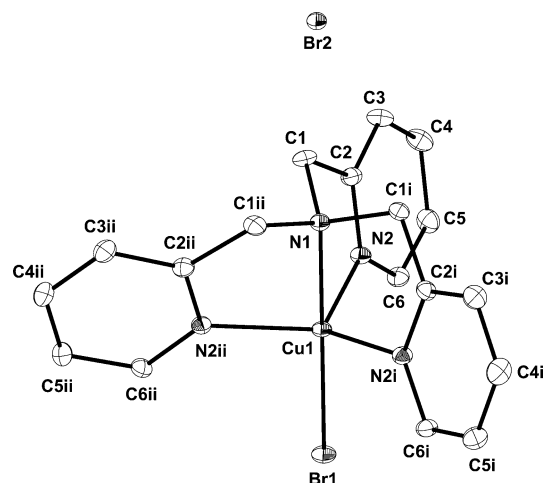


Figure 4. Molecular structure of the $[\text{Cu}^{\text{II}}(\text{TPMA})\text{Br}][\text{Br}]$, shown with 30% probability displacement ellipsoids. H atoms have been omitted for clarity. Symmetry codes: (i) $-y + 1/2, -z + 1, x + 1/2$ and (ii) $z - 1/2, -x + 1/2, -y + 1$. Selected distances (Å) and angles [°]: Cu1-N1 2.040(3), Cu1-N2 2.073(2), Cu1-Br1 2.3836(6), N1-Cu1-N2 80.86(5), $\text{N2-Cu1-N2}^{\text{i}}$ 117.53(3), N1-Cu1-Br1 180.00(5).

were also made in the case of $\text{Cu}^{\text{I}}(\text{TPMA})\text{Cl}$ and $[\text{Cu}^{\text{II}}(\text{TPMA})\text{Cl}][\text{Cl}]$ complexes, in which the shortening of $\text{Cu}\text{-N}_{\text{ax}}$ bond length on going from copper(I) to copper(II) complex was determined to be 0.389 Å.^[27] From the structural point of view, the high activity of $\text{Cu}^{\text{I}}(\text{TPMA})\text{Br}$ and $[\text{Cu}^{\text{II}}(\text{TPMA})\text{Br}][\text{Br}]$ complexes in ATRA, can be explained by the fact that minimum entropic rearrangement is required when $\text{Cu}^{\text{I}}(\text{TPMA})\text{Br}$ complex homolytically cleaves R-Br bond to generate $[\text{Cu}^{\text{II}}(\text{TPMA})\text{Br}][\text{Br}]$. At the present moment, it is unclear what is the role of Br^- coordination to the $[\text{Cu}^{\text{I}}(\text{TPMA})]^+$ cation [$\text{Cu}\text{-Br} = 2.5088(3)$ Å]. The most reasonable explanation is that the activation in ATRA/ATRP process proceeds with either prior dissociation of Br^- from $\text{Cu}^{\text{I}}(\text{TPMA})\text{Br}$ complex or dissociation of Br^- from the corresponding $\text{Cu}^{\text{II}}(\text{TPMA})\text{Br}_2$ to generate the deactivator $[\text{Cu}^{\text{II}}(\text{TPMA})\text{Br}][\text{Br}]$. As a part of an ongoing investigation in our laboratories, detailed kinetic measurements and cyclic voltammetry studies are being conducted in order to further investigate the equilibrium for Br^- coordination to the $[\text{Cu}^{\text{I}}(\text{TPMA})]^+$ cation in $\text{Cu}^{\text{I}}(\text{TPMA})\text{Br}$ complex and its effect on catalytic activity and reaction mechanism.

Conclusions

In summary, the synthesis, characterization and high activity of $\text{Cu}^{\text{I}}\text{Br}$ and $\text{Cu}^{\text{II}}\text{Br}_2$ complexes with TPMA in ATRA of polybrominated compounds to alkenes was reported. The methodology utilized AIBN, which provided external source of radicals for continuous regeneration of the copper(I) complex. $[\text{Cu}^{\text{II}}(\text{TPMA})\text{Br}][\text{Br}]$, in conjunction with AIBN, effectively catalyzed ATRA reactions of CBr_4 and CHBr_3 to alkenes with concentrations between 5 and 100 ppm, which is the lowest number achieved in copper-mediated ATRA. Molecular structure of $\text{Cu}^{\text{I}}(\text{TPMA})\text{Br}$

indicated that the complex was pseudo-pentacoordinate in the solid state due to the coordination of the bromide anion to the copper(I) center [Cu^I–Br 2.5088(3) Å]. Variable temperature ¹H NMR and cyclic voltammetry studies confirmed the equilibrium between Cu^I(TPMA)Br and [Cu^I(TPMA)(S)]Br (S = solvent) complexes, indicating halide anion dissociation in solution. The extent of dissociation was dependent on the solvent polarity and temperature. In [Cu^{II}(TPMA)Br][Br], the Cu^{II} atom was coordinated by four nitrogen atoms [Cu^{II}–N_{eq} 2.073(2) Å and Cu^{II}–N_{ax} 2.040(3) Å] from TPMA ligand and a bromine atom [Cu^{II}–Br 2.3836(6) Å]. The overall geometry of the complex was distorted trigonal bipyramidal. Cu^I(TPMA)Br and [Cu^{II}(TPMA)Br][Br] complexes showed similar structural features for the point of view of TPMA coordination. The only more pronounced difference in the TPMA coordination to the copper center was observed in the shortening of Cu–N_{ax} bond length by approximately 0.400 Å on going from Cu^I(TPMA)Br to [Cu^{II}(TPMA)Br][Br]. Apart from the detailed structural and mechanistic studies of this interesting catalytic system, we are presently utilizing the outlined procedure to decrease the amount of copper catalyst in synthetically more attractive atom transfer radical cyclization (ATRC) reactions.

Experimental Section

General Procedures: All chemicals were purchased from commercial sources and used as received. Tris(2-pyridylmethyl)amine (TPMA) was synthesized according to literature procedures.¹⁶⁵ Solvents (dichloromethane, pentane, acetonitrile and toluene) were degassed and deoxygenated using Innovative Technology solvent purifier. All monomers were degassed by bubbling argon for 30 min and stored in the dry box. Methanol was distilled and deoxygenated by bubbling argon for 30 min prior to use. All manipulations were performed under argon in a dry box (<1.0 ppm of O₂ and <0.5 ppm of H₂O) or using standard Schlenk line techniques. ¹H NMR spectra were obtained with Bruker Avance 300 and 400 MHz spectrometers and chemical shifts are given in ppm relative to residual solvent peaks [C₆D₆, 7.16 ppm; CDCl₃, 7.26 ppm; (CD₃)₂CO, 2.05 ppm]. IR spectra were recorded in the solid state or in solution with a Nicolet Smart Orbit 380 FT-IR spectrometer (Thermo Electron Corporation). Elemental analyses for C, H and N were obtained from Midwest Microlab, LLC.

Synthesis of Cu^I(TPMA)Br: Cu^IBr (25.0 mg, 0.174 mmol) and TPMA (50.0 mg, 0.174 mmol) were dissolved in 2 mL of EtOH/THF (50%/50% vol.) and slow crystallization at –35 °C afforded orange crystals. The supernatant liquid was decanted and the crystals washed with 2 × 10 mL *n*-pentane and dried under vacuum to yield 47 mg (63%) of Cu^I(TPMA)Br. ¹H NMR [(CD₃)₂CO, 300 MHz, 220 K]: δ = 9.10 (d, *J* = 4.2 Hz, 3 H), 7.81 (dt, *J*₁ = 7.7, *J*₂ = 1.8 Hz, 3 H), 7.36 (d, *J* = 7.8 Hz, 3 H), 7.32 (m, 3 H), 3.94 (s, 6 H) ppm. C₁₈H₁₈BrCuN₄ (433.81): calcd. C 49.84, H 4.18, N 12.91; found C 49.55, H 4.09, N 12.65.

Synthesis of [Cu^{II}(TPMA)Br][Br]: Dichloromethane (2 mL) was added to a round-bottomed flask containing Cu^{II}Br₂ (0.878 g, 3.93 mmol) and tris(2-pyridylmethyl)amine (TPMA) (1.141 g, 3.93 mmol). The reaction mixture was stirred at room temperature for 30 min and the product precipitated by the slow addition of *n*-pentane. The supernatant liquid was decanted and the green pow-

der was washed with 2 × 10 mL of *n*-pentane and dried under vacuum to yield 1.93 g (96%) of [Cu^{II}(TPMA)Br][Br]. C₁₈H₁₈Br₂CuN₄ (513.72): calcd. C 42.08, H 3.53, N 10.91; found C 42.06, H 3.55, N 10.72. FT-IR (solid): $\tilde{\nu}$ = 3048 (w), 2932, (w), 2864 (w), 1602 (m), 1470 (m), 1434 (m), 1299 (m), 1155 (w), 1091 (m), 1016 (m), 792 (s), 648 (m) cm⁻¹. Crystals suitable for X-ray analysis were obtained by slow diffusion of diethyl ether into an acetonitrile solution of the complex at room temperature.

Catalyst Solutions: Two catalyst solutions were made using dilution flasks to accommodate the various catalyst loadings. Catalyst solution A was made by dissolving 25.7 mg of [Cu(TPMA)Br][Br] in 5.00 mL of acetonitrile to give a 0.01 M solution. Catalyst solution B was made in two steps by first dissolving 25.7 mg of [Cu(TPMA)Br][Br] in 10.00 mL of acetonitrile to give a 0.005 M solution. 1.00 mL of this 0.005 M solution was then diluted to 10.00 mL of acetonitrile to yield a 0.0005 M catalyst solution.

ATRA of CHBr₃ to Alkenes: To a 5-mL Schlenk flask was added bromoform (282.0 μL, 3.22 mmol), which was dissolved in 500 μL of acetonitrile. To this solution was added alkene (0.805 mmol), AIBN (6.6 mg, 40.3 μmol), and toluene (15.0 μL) in the case of 1-hexene, 1-octene, and 1-decene or anisole in the case of styrene and methyl acrylate. The catalyst solution A was then added at the desired alkene/catalyst ratio between 500:1 and 10000:1. The flask was then sealed under argon and stirred at 60 °C for 24 h. The conversion of the alkene and the yield of the monoadduct was determined by ¹H NMR using internal standard. Column chromatography was used to determine isolated yields (10% ethyl acetate in hexanes for styrene and methyl acrylate and hexane for 1-hexene, 1-octene, and 1-decene).

ATRA of CBr₄ to Alkenes: Carbon tetrabromide (1.067 g, 3.22 mmol) was placed in a 5-mL Schlenk flask and dissolved in 500.0 μL of acetonitrile. Alkene (0.805 mmol), AIBN (6.6 mg, 40.3 μmol), and toluene (15.0 μL) was added to this solution in the case of 1-hexene, 1-octene, and 1-decene or anisole in the case of styrene and methyl acrylate. The catalyst solution B was then added at the desired alkene/catalyst ratio between 100000:1 and 200000:1. The flask was then sealed under argon and stirred at 60 °C for 24 h. The conversion of the alkene and the yield of the monoadduct was determined by ¹H NMR using internal standard. Column chromatography was used to determine isolated yields (10% ethyl acetate in hexanes for styrene and methyl acrylate and hexane for 1-hexene, 1-octene, and 1-decene).

X-ray Crystal Structure Determination: The X-ray intensity data were collected at 150 K using graphite-monochromated Mo-*K*_α radiation (λ = 0.71073 Å) with a Bruker Smart Apex II CCD diffractometer. Data reduction included absorption corrections by the multiscan method using SADABS.¹⁶⁶ Crystal data and experimental conditions are given in Table 4. Structures were solved by direct methods and refined by full-matrix least-squares using SHELXTL 6.1 bundled software package.¹⁶⁷ The H atoms were positioned geometrically (aromatic C–H 0.93 Å, methylene C–H 0.97 Å and methyl C–H 0.96 Å) and treated as riding atoms during subsequent refinement, with *U*_{iso}(H) = 1.2*U*_{eq}(C) or 1.5*U*_{eq}(methyl C). The methyl groups were allowed to rotate about their local threefold axes. ORTEP-3 for Windows and Crystal Maker 7.2 were used to generate molecular graphics.¹⁶⁸

CCDC-649993 [for Cu^I(TPMA)Br] and -649992 {for [Cu^{II}(TPMA)Br][Br]} contain the supplementary crystallographic data for this paper. These data can be obtained free of charge from The Cambridge Crystallographic Data Centre via www.ccdc.cam.ac.uk/data_request/cif.

Table 4. Crystallographic data and experimental details for Cu^I(TPMA)Br and [Cu^{II}(TPMA)Br][Br].

	Cu ^I (TPMA)Br	[Cu ^{II} (TPMA)Br][Br]
Empirical formula	C ₁₈ H ₁₈ BrCuN ₄	C ₁₈ H ₁₈ Br ₂ CuN ₄
Color/shape	orange/needles	green/rhomboids
Formula weight	433.81	513.72
Crystal system	monoclinic	cubic
Space group	<i>P</i> 21/ <i>c</i>	<i>P</i> 21 3
Temperature [K]	150(2)	150(2)
Cell constants		
<i>a</i> [Å]	10.3042(9)	12.6335(3)
<i>b</i> [Å]	14.2256(12)	12.6335(3)
<i>c</i> [Å]	12.5491(11)	12.6335(3)
<i>a</i> [°]	90	90
<i>β</i> [°]	105.5800(10)	90
<i>γ</i> [°]	90	90
<i>V</i> (Å ³)	1771.9(3)	2016.37(8)
Formula units/unit cell	4	4
$\rho_{\text{calcd.}}$ [gcm ⁻³]	1.626	1.692
Absorption coefficient [mm ⁻¹]	3.494	5.054
Diffractometer	Bruker Smart Apex II	Bruker Smart Apex II
Radiation, graphite-monochromated	Mo- <i>K</i> _α ($\lambda = 0.71073$ Å)	Mo- <i>K</i> _α ($\lambda = 0.71073$ Å)
Crystal size [mm]	0.41 × 0.14 × 0.03	0.26 × 0.14 × 0.09
θ range [°]	2.05 to 32.25	2.28 to 32.81
Range of <i>h, k, l</i>	±15, -21 → 20, ±18	±18, -18 → 19, -19 → 18
Reflections collected/unique	23037/6166	26426/2460
<i>R</i> _{int}	0.0390	0.1665
Refinement method	full-matrix least-squares on <i>F</i> ²	full-matrix least-squares on <i>F</i> ²
Data/restraints/parameters	6166/0/217	2460/0/76
Goodness-of-fit on <i>F</i> ²	1.015	1.030
Final <i>R</i> indices [<i>I</i> > 2σ(<i>I</i>)]	<i>R</i> ₁ = 0.0304, <i>wR</i> ₂ = 0.0621	<i>R</i> ₁ = 0.0271, <i>wR</i> ₂ = 0.0637
<i>R</i> indices (all data)	<i>R</i> ₁ = 0.0511, <i>wR</i> ₂ = 0.0680	<i>R</i> ₁ = 0.0343, <i>wR</i> ₂ = 0.0649
Max. resid. peaks [e Å ⁻³]	0.450 and -0.357	0.566 and -0.544

Cyclic Voltammetry: Electrochemical measurements were carried out using Bioanalytical Systems (BAS) model CV-50W in a dry box. Cyclic voltammograms were recorded with a standard three-electrode system consisting of a Pt-wire working electrode, a standard calomel reference electrode, and a Pt-wire auxiliary electrode. Tetrabutylammonium perchlorate (TBAClO₄), tetrabutylammonium hexafluorophosphate (TBAPF₆) and tetrabutylammonium bromide (TBABr) were used as the supporting electrolyte, and all voltammograms were externally referenced to ferrocene. As such, the potentials are reported with respect to Fc/Fc⁺ couple, without junction correction. All cyclic voltammograms were simulated digitally to obtain the half-wave potentials.

Acknowledgments

Financial support from Duquesne University (start-up grant and faculty development grant), National Science Foundation X-ray facility grant (NSF CRIF 0234872), and National Science Foundation NMR grant (NSF CHE 0614785) is gratefully acknowledged.

- [1] D. P. Curran, *Synthesis* **1988**, 6, 417–439.
- [2] D. P. Curran, *Synthesis* **1988**, 7, 489–513.
- [3] M. S. Kharasch, E. V. Jensen, W. H. Urry, *Science* **1945**, 102, 128.
- [4] M. S. Kharasch, E. V. Jensen, W. H. Urry, *J. Am. Chem. Soc.* **1945**, 67, 1626.
- [5] D. P. Curran, *Comprehensive Organic Synthesis*, Pergamon, New York, **1992**.
- [6] J. Iqbal, B. Bhatia, N. K. Nayyar, *Chem. Rev.* **1994**, 94, 519–564.
- [7] K. Severin, *Curr. Org. Chem.* **2006**, 10, 217–224.
- [8] R. A. Gossage, L. A. Van De Kuil, G. Van Koten, *Acc. Chem. Res.* **1998**, 31, 423–431.
- [9] A. J. Clark, *J. Chem. Soc. Rev.* **2002**, 31, 1–11.
- [10] J. S. Wang, K. Matyjaszewski, *J. Am. Chem. Soc.* **1995**, 117, 5614–5615.
- [11] K. Matyjaszewski, J. Xia, *Chem. Rev.* **2001**, 101, 2921–2990.
- [12] K. Matyjaszewski (Ed.), *Controlled Radical Polymerization (ACS Symp. Ser. 685)*, ACS, Washington, DC, **1998**.
- [13] K. Matyjaszewski (Ed.), *Controlled/Living Radical Polymerization. Progress in ATRP, NMP and RAFT (ACS Symp. Ser. 768)*, ACS, Washington, DC, **2000**.
- [14] V. Coessens, T. Pintauer, K. Matyjaszewski, *Prog. Polym. Sci.* **2001**, 26, 337.
- [15] K. Matyjaszewski, T. P. Davis (Eds.), *Handbook of Radical Polymerization*, Wiley, Hoboken, **2002**.
- [16] K. Matyjaszewski (Ed.), *Advances in Controlled/Living Radical Polymerization (ACS Symp. Ser. 854)*, ACS, Washington, DC, **2003**.
- [17] K. Matyjaszewski, *Macromol. Symp.* **2003**, 195, 25–31.
- [18] K. Matyjaszewski, *Prog. Polym. Sci.* **2005**, 30, 858–875.
- [19] K. Matyjaszewski (Ed.), *Controlled Radical Polymerization. From Synthesis to Materials (ACS Symp. Ser. 944)*, ACS, Washington, DC, **2006**.
- [20] T. E. Patten, K. Matyjaszewski, *Acc. Chem. Res.* **1999**, 32, 895–903.
- [21] M. Kamigaito, T. Ando, M. Sawamoto, *Chem. Rev.* **2001**, 101, 3689–3745.
- [22] K. Matyjaszewski, W. Jakubowski, K. Min, W. Tang, J. Huang, W. A. Braunecker, N. V. Tsarevsky, *Proc. Natl. Acad. Sci. USA* **2006**, 103, 15309–15314.
- [23] W. Jakubowski, K. Matyjaszewski, *Angew. Chem. Int. Ed.* **2006**, 45, 4482–4486.
- [24] W. Jakubowski, K. Min, K. Matyjaszewski, *Macromolecules* **2006**, 39, 39–45.

- [25] L. Quebatte, K. Thommes, K. Severin, *J. Am. Chem. Soc.* **2006**, *128*, 7440–7441.
- [26] K. Thommes, B. Icli, R. Scopelliti, K. Severin, *Chem. Eur. J.* **2007**, *13*, 6899–6907.
- [27] W. T. Eckenhoff, T. Pintauer, *Inorg. Chem.* **2007**, *46*, 5844–5846.
- [28] J. Xia, S. G. Gaynor, K. Matyjaszewski, *Macromolecules* **1998**, *31*, 5958–5959.
- [29] J. Xia, K. Matyjaszewski, *Macromolecules* **1999**, *32*, 2434–2437.
- [30] H. Tang, N. Arulsamy, M. Radosz, Y. Shen, N. V. Tsarevsky, W. A. Braunecker, W. Tang, K. Matyjaszewski, *J. Am. Chem. Soc.* **2006**, *128*, 16277–16285.
- [31] F. Minisci, *Acc. Chem. Res.* **1975**, *8*, 165–171.
- [32] M. Asscher, D. Vofsi, *J. Chem. Soc.* **1961**, 2261–2264.
- [33] L. Delaude, A. Demonceau, A. F. Noels, in *Topics in Organometallic Chemistry*, vol. 11 (Eds.: C. Bruneau, P. H. Dixneuf), Springer, Berlin, **2004**, pp. 155–171.
- [34] H. Nagashima, in *Ruthenium in Organic Synthesis* (Ed.: S.-I. Murahashi), Wiley-VCH, Weinheim, **2004**, pp. 333–343.
- [35] C. P. Jasperse, D. P. Curran, T. L. Fevig, *Chem. Rev.* **1991**, *91*, 1237–1286.
- [36] B. Giese, *Angew. Chem.* **1985**, *97*, 555.
- [37] D. P. Curran, M.-H. Chen, E. Spletzer, C. M. Seong, C.-T. Chang, *J. Am. Chem. Soc.* **1986**, *108*, 6384.
- [38] J. Brandrup, E. H. Immergut, E. A. Gulke, *Polymer Handbook*, Wiley Interscience, New York, **1999**.
- [39] G. C. Eastmond, in *Comprehensive Chemical Kinetics*, vol. 14A (Eds.: C. H. Bamford, C. F. H. Tipper), American Elsevier, New York, **1976**.
- [40] F. De Campo, D. Lastecoueres, J.-B. Verlhac, *J. Chem. Soc. Perkin Trans. 1* **2000**, 575–580.
- [41] J. M. Munoz-Molina, A. Caballero, M. M. Diaz-Requejo, S. Trofimenko, T. R. Belderrain, P. J. Perez, *Inorg. Chem.* **2007**, *46*, 7725–7730.
- [42] W. Tang, N. V. Tsarevsky, K. Matyjaszewski, *J. Am. Chem. Soc.* **2006**, *128*, 1598–1604.
- [43] K. Matyjaszewski, H.-j. Paik, P. Zhou, S. J. Diamanti, *Macromolecules* **2001**, *34*, 5125–5131.
- [44] K. Matyjaszewski, B. Gobelt, H.-j. Paik, C. P. Horwitz, *Macromolecules* **2001**, *34*, 430–440.
- [45] M. A. J. Schellekens, F. de Wit, B. Klumperman, *Macromolecules* **2001**, *34*, 7961–7966.
- [46] T. Pintauer, K. Matyjaszewski, *Coord. Chem. Rev.* **2005**, *249*, 1155–1184.
- [47] K. D. Karlin, J. Zubieta, *Copper Coordination Chemistry: Biochemical and Inorganic Perspectives*, Adenine Press, New York, **1983**.
- [48] M. Becker, F. W. Heinemann, S. Schindler, *Chem. Eur. J.* **1999**, *5*, 3124–3129.
- [49] G. Kickelbick, T. Pintauer, K. Matyjaszewski, *New J. Chem.* **2002**, *26*, 462–468.
- [50] T. Pintauer, B. McKenzie, K. Matyjaszewski, *ACS. Symp. Ser.* **2003**, *854*, 130–147.
- [51] T. Pintauer, U. Reinohl, M. Feth, H. Bertagnolli, K. Matyjaszewski, *Eur. J. Inorg. Chem.* **2003**, 2082–2094.
- [52] G. Wilkinson, *Comprehensive Coordination Chemistry*, Vol. 5, Pergamon Press, New York, **1987**.
- [53] M. Munakata, S. Kitagawa, S. Kosome, A. Asahara, *Inorg. Chem.* **1986**, *25*, 2622–2627.
- [54] J. S. Thompson, R. M. Swiatek, *Inorg. Chem.* **1985**, *24*, 110–113.
- [55] S. Kitagawa, M. Munakata, *Inorg. Chem.* **1981**, *20*, 2261–2267.
- [56] S. Kitagawa, M. Munakata, N. Miyaji, *Inorg. Chem.* **1982**, *21*, 3842–3843.
- [57] C. Mealli, C. A. Arcus, J. L. Wilkinson, T. J. Marks, J. A. Ibers, *J. Am. Chem. Soc.* **1976**, *98*, 711–718.
- [58] D. K. Coggin, J. A. Gonzalez, A. M. Kook, D. M. Stanbury, L. J. Wilson, *Inorg. Chem.* **1991**, *30*, 1115–1125.
- [59] S. M. Carrier, C. E. Ruggiero, R. P. Houser, W. B. Tolman, *Inorg. Chem.* **1993**, *32*, 4889–4899.
- [60] C. X. Zhang, S. Kaderli, M. Costas, E.-I. Kim, Y.-M. Neuhold, K. D. Karlin, A. D. Zuberbuhler, *Inorg. Chem.* **2003**, *42*, 1807–1824.
- [61] Z. Tyeklar, R. R. Jacobson, N. Wei, N. N. Murthy, J. Zubieta, K. D. Karlin, *J. Am. Chem. Soc.* **1993**, *115*, 2677–2689.
- [62] N. V. Tsarevsky, K. Matyjaszewski, *Chem. Rev.* **2007**, *107*, 2270–2299.
- [63] W. A. Braunecker, K. Matyjaszewski, *Prog. Polym. Sci.* **2007**, *32*, 93–146.
- [64] J. Qiu, K. Matyjaszewski, L. Thounin, C. Amatore, *Macromol. Chem. Phys.* **2000**, *201*, 1625–1631.
- [65] Z. Tyeklar, R. R. Jacobson, N. Wei, N. N. Murthy, J. Zubieta, K. D. Karlin, *J. Am. Chem. Soc.* **1993**, *115*, 2677–2689.
- [66] G. M. Sheldrick, *SADABS Version 2.03*, University of Göttingen, Germany, **2002**.
- [67] G. M. Sheldrick, *SHELXTL 6.1, Crystallographic Computing System*, Bruker Analytical X-ray System, Madison, WI, **2000**.
- [68] L. J. Farrugia, *J. Appl. Crystallogr.* **1997**, *30*, 565.

Received: October 22, 2007

Published Online: December 3, 2007